Archival Report

Biological Psychiatry

Presynaptic D_2 Dopamine Receptors Control Long-Term Depression Expression and Memory Processes in the Temporal Hippocampus

Jill Rocchetti, Elsa Isingrini, Gregory Dal Bo, Sara Sagheby, Aurore Menegaux, François Tronche, Daniel Levesque, Luc Moquin, Alain Gratton, Tak Pan Wong, Marcelo Rubinstein, and Bruno Giros

ABSTRACT

BACKGROUND: Dysfunctional mesocorticolimbic dopamine signaling has been linked to alterations in motor and reward-based functions associated with psychiatric disorders. Converging evidence from patients with psychiatric disorders and use of antipsychotics suggests that imbalance of dopamine signaling deeply alters hippocampal functions. However, given the lack of full characterization of a functional mesohippocampal pathway, the precise role of dopamine transmission in memory deficits associated with these disorders and their dedicated therapies is unknown. In particular, the positive outcome of antipsychotic treatments, commonly antagonizing D_2 dopamine receptors (D2Rs), on cognitive deficits and memory impairments remains questionable.

METHODS: Following pharmacologic and genetic manipulation of dopamine transmission, we performed anatomic, neurochemical, electrophysiologic, and behavioral investigations to uncover the role of D2Rs in hippocampal-dependent plasticity and learning. Naïve mice (n = 4–21) were used in the different procedures.

RESULTS: Dopamine modulated both long-term potentiation and long-term depression in the temporal hippocampus as well as spatial and recognition learning and memory in mice through D2Rs. Although genetic deletion or pharmacologic blockade of D2Rs led to the loss of long-term potentiation expression, the specific genetic removal of presynaptic D2Rs impaired long-term depression and performances on spatial memory tasks.

CONCLUSIONS: Presynaptic D2Rs in dopamine fibers of the temporal hippocampus tightly modulate long-term depression expression and play a major role in the regulation of hippocampal learning and memory. This direct role of mesohippocampal dopamine input as uncovered here adds a new dimension to dopamine involvement in the physiology underlying deficits associated with neuropsychiatric disorders.

Keywords: Antipsychotics, D_2 dopamine receptors, LTD, Memory, Neuronal plasticity, Temporal hippocampus

http://dx.doi.org/10.1016/j.biopsych.2014.03.013

In addition to roles in motor and reward systems (1,2), dopamine has been acknowledged to be essential in adaptive behaviors, such as attention, learning, and memory (3–5). The development of powerful genetic tools has enabled a better understanding of the function of dopamine in the basal ganglia and the cortical structures (6) involved in these motor and reward functions. However, the limited innervation by dopamine terminals and the low levels of dopamine receptor expression in the hippocampus (7–9) have slowed efforts of understanding the potential role of dopamine in the mesohippocampal pathway (10). Considering the pathologic imbalance in hippocampal dopamine transmission observed in patients with schizophrenia (11–14) and the lack of perspective on the impact of antipsychotic treatments in memory processes, there is an urgent need to understand better the contribution of dopamine in hippocampal-related processes.

Long-term synaptic plasticity with its two counterparts, long-term potentiation (LTP) and long-term depression (LTD), underlies neuronal circuit tuning. It was shown 40 years ago via microelectrophoretic studies that application of dopamine in the hippocampal CA3 region of cats depressed glutamate-induced cell firing (15). However, how dopamine modulates glutamatergic transmission in the hippocampus is still poorly understood.

Five dopamine receptors have been identified in mammals (16) and classified into the D_1/D_5 (D_1-like) and D_2/D_3/D_4 (D_2-like) families. Both D_1-like and D_2-like dopamine receptor agonists and antagonists regulate synaptic plasticity (17); although the role of D_1 dopamine receptors (D1Rs) in hippocampal synaptic plasticity is well understood, little is known about the precise role of D_2 dopamine receptors (D2Rs). Blockade of D1Rs inhibits the expression and maintenance of late LTP (18–20), whereas the D1R agonist SKF-38393 favors the early and late phases of LTP (21,22). In D1R knockout mice, an absence of late LTP in vitro (23) and impaired spatial memory (24) were exhibited. Conversely, the

ISSN: 0006-3223

role of D2Rs in the hippocampus remains controversial. Activation of D2Rs exerted a suppressive effect on CA1 LTD in the rat hippocampus (25) with no effect on LTP (21), but D2R agonists directly administered in the hippocampus improved memory performance in radial maze tasks (26,27). Rats treated with the D2R antagonist haloperidol displayed spatial learning deficits (28,29) and impaired recognition memory (30,31). Systemic injection of the D_2/D_3 antagonist sulpiride affected learning in the spatial version of the Morris water maze (MWM) (32), but whether this reflected a specific effect on the hippocampus remains unclear (33).

Although D1Rs are present only on dopaminoceptive neurons, D2Rs are localized both postsynaptically, where they activate multiple signalization pathways (34), and presynaptically, where they exert an inhibitory control over dopamine synthesis and release (35,36). This dual localization of D2Rs potentially results in multimodal processes with complex effects.

In the present study, we showed that D2R postsynaptic expression was restricted to neurons of the dentate gyrus (DG), whereas dopamine fibers expressing the dopamine transporter (DAT) originating from the ventral tegmental area (VTA) and carrying presynaptic D2R innervated the temporal CA1 areas. The genetic deletion of D2Rs severely impairs both *N*-methyl-D-aspartate receptor (NMDAR)–dependent LTP and LTD in CA1, corresponding with remodeling of mesohippocampal dopamine fibers and decrease in performance on learning and memory tasks. The pharmacologic blockade of D2Rs in naïve mice reproduced these impairments. Finally, the specific genetic deletion of presynaptic D2Rs resulted in deficits of both LTD expression and spatial memory without impairing LTP levels.

METHODS AND MATERIALS

Detailed descriptions of procedures are provided in Supplement 1.

Animals

Mice with a constitutive deletion of D2Rs were acquired from Jackson Laboratories (Bar Harbor, Maine) (B6.129S2-Drd2^{tm1Low}/J). Mice expressing the recombinase cre in the D2 gene (D2cre) were acquired from Gensat [MMRC; B6.FVB(Cg)-Tg(Drd2-cre)$^{ER44Gsat/Mmucd}$] and crossed with mice carrying ROSA-tomato reporter acquired from Jackson Laboratories [Gt(ROSA)26Sor$^{tm9(CAG-tdTomato)Hze}$]. Mice with floxed D2R gene (36) and mice expressing the cre recombinase in a BAC-DAT transgene (DATcre mice) (37) were directly obtained from MR and FT animal facilities respectively.

Anatomic Procedures

Dopamine receptor messenger RNAs (mRNAs) were detected by radioactive and fluorescent in situ hybridization. Immunolabeling was adapted from a previous protocol to detect DAT, Ca2+/calmodulin-dependent protein kinase II-α (CaMK2α), tyrosine hydroxylase (TH), and gamma-aminobutyric acid (GABA) on coronal slices from D_2 knockout (D2KO), D2^{DATcre}, and sulpiride-treated mice. All experiments were performed on naïve mice (n = 4–10) (Table S1 in Supplement 1).

Electrophysiologic Recordings

Field excitatory postsynaptic potentials and whole-cell patch-clamp recordings were performed on coronal slices prepared from D2KO, D2^{DATcre}, and C57BL/6 wild-type (WT) mice in the presence of sulpiride or the D1R antagonist SCH23390. All experiments were performed in the presence of 5 μmol/L bicuculline. All experiments were performed on naïve mice (n = 6–11) (Table S2 in Supplement 1).

Behavioral Tests

Male D2KO and D2^{DATcre} sulpiride-treated (intraperitoneal injection 50 mg/kg; intrahippocampal injection 2.5 μg) mice and respective control mice were exposed to spatial and cued versions of the MWM, Barnes maze, two-object recognition task, and contextual and cued fear conditioning. All experiments were performed on naïve mice (n = 9–21) (Table S3 in Supplement 1).

Statistical Comparisons

Results are reported as mean ± SEM. Statistical analyses were done with Student t test and analysis of variance, unless otherwise specified (Tables S1–S3 in Supplement 1).

RESULTS

Mapping of Dopamine Receptors and Fibers in Hippocampal Formation

The distribution of the five dopamine receptors was evaluated by in situ hybridization in C57BL/6J mouse brains (Figure 1A–C; Figure S1 in Supplement 1). The expression of D_3 dopamine receptor mRNA and D_4 dopamine receptor mRNA in the hippocampus (Figure S1B,C in Supplement 1) fell below our detection limit (Figure S1B in Supplement 1). The expression of D1R mRNA was restricted to the granular cell layer of the DG (Figure S1A in Supplement 1), and the expression of D2R mRNA was observed only in the polymorphic layer (hilus) of the DG (Figure 1A,B). D_5 dopamine receptor mRNA was expressed in granular and pyramidal cell layers (Figure S1D in Supplement 1). Radiolabeling with [^{125}I]-iodosulpride detected the presence of D2R in the granular cell layer, in addition to the polymorphic layer of the DG (Figure 1D,E). The specificity of D2R expression was shown using D2KO mice (Figure 1C–F). Combined D2R fluorescent in situ hybridization and immunolabeling against CaMK2α showed the D2R-expressing neurons in the hilus to be glutamatergic (Figure 1G–I; Figure S1E–H in Supplement 1). Using reporter tdTomato^{D2cre} mice, we identified these neurons as mossy neurons, given their morphology and their projection patterns (Figure 1J).

Because most of the TH labeling found in the hippocampus originates from noradrenergic neurons (38), we visualized dopamine transporter–positive (DAT$^+$) fibers to characterize the dopamine projections. The DAT$^+$ fibers were restricted to the temporal area of CA1 (Figure 1K,L) and totally absent in the septal part of the hippocampus (Figure S2A,B in Supplement 1). The strongest labeling was observed in the dorsal part of the stratum radiatum and the ventral part of the laconosum moleculare layer of CA1 (Figure S2C,D in Supplement 1). The specificity of DAT labeling was confirmed using DAT knockout mice (Figure S2E in Supplement 1) (38).

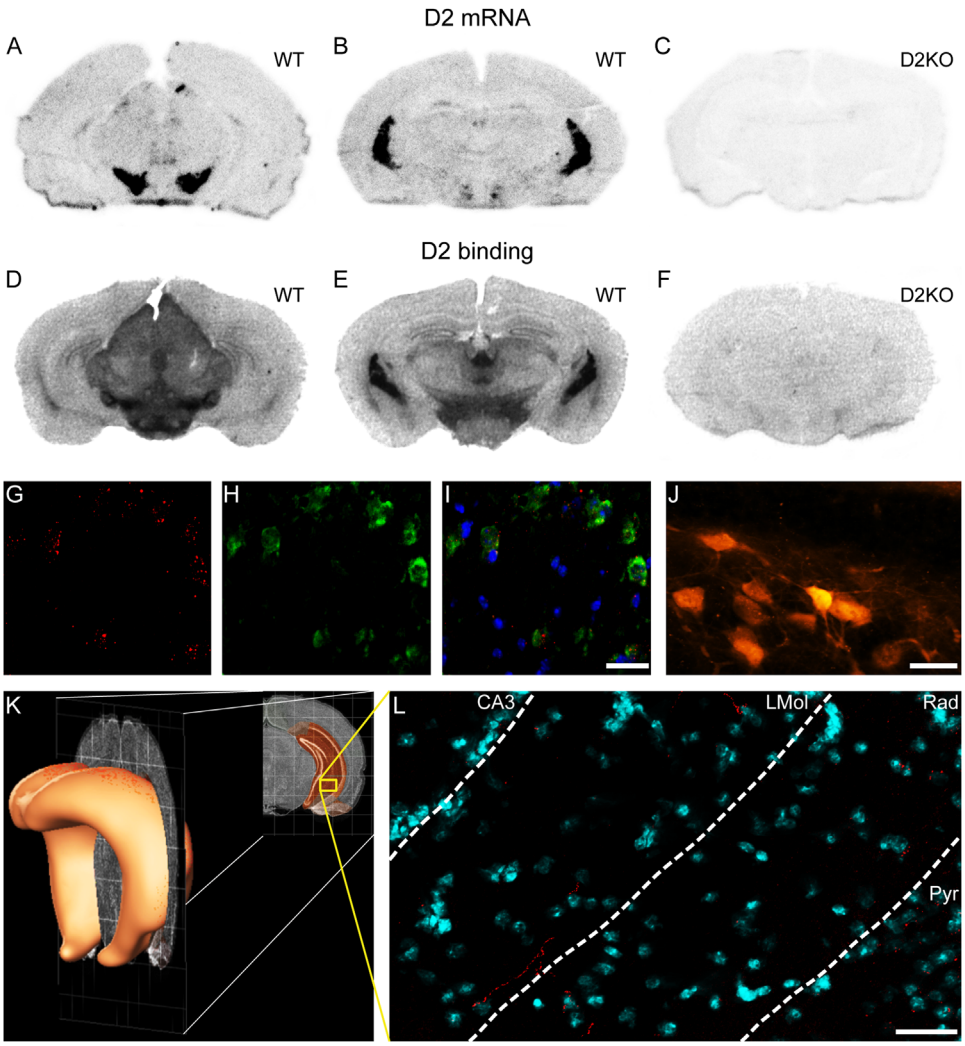

Figure 1. Dopamine D_2 receptor (D2R) and dopamine fiber distribution in the hippocampus. **(A–C)** D2R messenger RNA (mRNA) expression detected by antisense [^{35}S]-oligonucleotides in hippocampus of wild-type (WT) mice **(A,B)** was restricted to the polymorphic layer of dentate gyrus along the anteroposterior axis. No signal was detected on coronal slices from D_2 knockout (D2KO) mice **(C). (D–F)** Autoradiographic detection of D2Rs using [^{125}I]-iodosulpride labeling in the granular layer of the dentate gyrus and in the proximal pyramidal cells of CA3 in WT mice **(D,E)** with no signal in the D2KO slices **(F). (G–I)** Fluorescent in situ hybridization for D2R mRNA (**G**, red) coupled to immunolabeling for CaMK2α (**H**, green) in mossy cells of the dentate gyrus with Hoechst staining (**I**, blue). (Scale bar = 25 μm.) **(J)** Morphologic confirmation of mossy cells expressing D2Rs in D2-tomato reporter mice. (Scale bar = 25 μm.) **(K)** Schematic three-dimensional representation of hippocampus with representation of coronal sections within temporal hippocampus (anterior to bregma, −3.2 mm). **(L)** Immunolabeling for dopamine transporter–positive (red) fibers restricted in CA1 division of hippocampus. Slices were counterstained with Hoechst staining (blue). (Scale bar = 50 μm.) LMol, laconosum moleculare layer; Pyr, pyramidal layer; Rad, stratum radiatum.

Constitutive Deletion of D2Rs Led to Profound Remodeling of VTA-Hippocampus Dopaminergic Pathway

Compared with WT mice, D2KO mice had threefold to sevenfold more DAT$^+$ fibers in the hippocampus (Figure 2A–C). In the laconosum moleculare layer of CA1, D2KO mice showed a threefold increase in DAT$^+$ fibers (n = 4; 337 ± 52) compared with WT mice (n = 4; 111 ± 30). The radiatum layer showed a similar increase (308 ± 50 in D2KO mice; 85 ± 12 in D2WT mice), and a major sprouting was observed in the oriens and pyramidal cell layers, with sevenfold more DAT$^+$ fibers (257 ± 42) in D2KO than in D2WT mice (38 ± 9). Although DAT$^+$ fibers were absent in the hilus of the DG in D2WT mice, they were visible in D2KO mice (32.3 ± 12.2). No DAT$^+$ fibers were observable in any other subdivisions of the temporal hippocampus or in septal areas.

To determine the origin of the increase in DAT$^+$ fibers, we injected fluorescent RetroBeads (Lumafluor, Durham, North Carolina) into the CA1 of D2KO and D2WT mice (Figure 2C,D; Figure S2E,E′,E″ in Supplement 1). Most retrogradely labeled neurons were localized in the VTA (87%–89%); only a fraction of them were dopaminergic (16%–21%), whereas most were GABAergic (79%–84%). The number (n = 27) and the proportion (21%) of TH-positive neurons in D2KO mice were slightly increased compared with WT (n = 22; 16%). This increase did not account for the massive sprouting observed in D2KO hippocampus. Dopamine levels in the temporal hippocampus were significantly higher in D2KO mice (293.9 ± 30.9 ng/g) compared with D2WT mice (169.9 ± 21.4 ng/g) (Figure 2E; Figure S2G in Supplement 1). Finally, we assessed by microdialysis whether this increased sprouting of dopamine terminals in temporal hippocampus would translate into an increase in potassium chloride–induced dopamine release (Figure 2F; Figure S2F in Supplement 1). Basal levels of extracellular dopamine were similar in D2WT and D2KO mice. However, potassium chloride–induced paired depolarization led to 2.4 times greater dopamine release in the D2KO mice (K1 = 23.0 ± 6.3 ng/mL; K2 = 31.5 ± 10.4 ng/mL) compared with WT littermates (K1 = 11.2 ± 2.2; K2 = 13.05 ± 2.6). The second potassium chloride–induced stimulation (K2) in D2KO

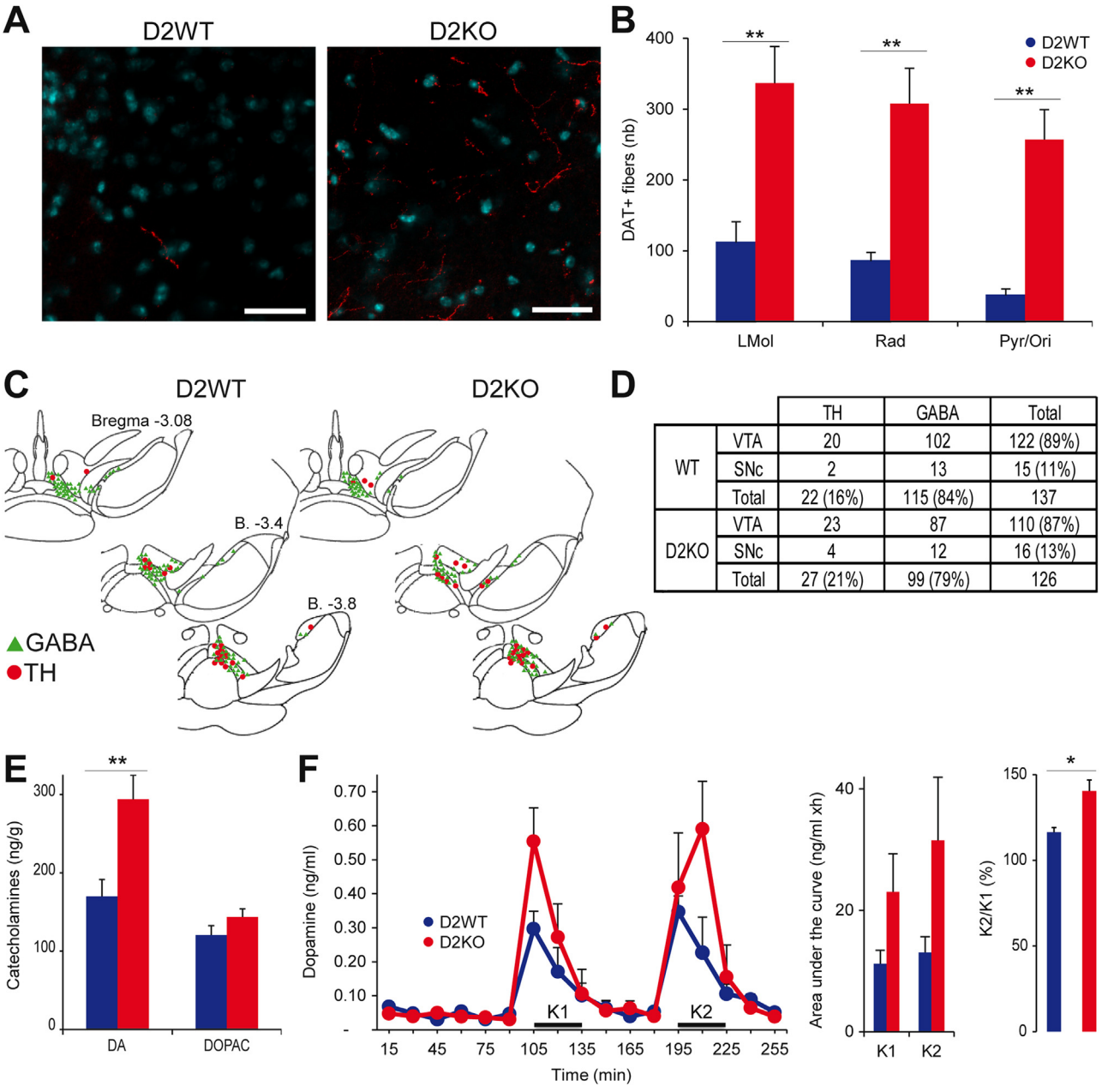

		TH	GABA	Total
WT	VTA	20	102	122 (89%)
	SNc	2	13	15 (11%)
	Total	22 (16%)	115 (84%)	137
D2KO	VTA	23	87	110 (87%)
	SNc	4	12	16 (13%)
	Total	27 (21%)	99 (79%)	126

Figure 2. Anatomic and physiologic characterizations of hyperdopaminergia in D_2 knockout (D2KO) mice. **(A)** Immunolabeling of dopamine transporter–positive fibers (red) in the stratum radiatum layer of the hippocampus of D_2 wild-type (D2WT) and D2KO mice. Coronal slices containing the hippocampus were counterstained with Hoescht (blue). (Scale bars = 50 μm.) **(B)** Quantification of dopamine transporter–positive (DAT^+) fibers in CA1 layers of the right hippocampus in D2WT and D2KO mice (n = 4 for each group; compared with D2WT, $^{**}p < .01$). **(C)** Schematic representations of retrolabeled neuron distribution in ventral mesencephalon of D2WT (left) and D2KO (right) mice. **(D)** Table compiling the numbers and the proportion of dopaminergic or GABAergic neurons retrogradely labeled in ventral tegmental area (VTA) or substantia nigra pars compacta (SNc) in D2WT (n = 10) and D2KO (n = 10) mice. **(E)** High-pressure liquid chromatography analysis of tissue catecholamine (dopamine [DA] and 3,4-dihydroxyphenylacetic acid [DOPAC]) levels in the hippocampus of D2WT (n = 10) and D2KO (n = 9) mice (compared with D2WT, $^{**}p < .01$). **(F)** Graph on the left demonstrates microdialysis analysis of extracellular dopamine in the right temporal hippocampus of D2WT and D2KO mice (n = 6 per group) at baseline and during two potassium chloride stimulations (K1, K2). Center graph demonstrates area under the curve during potassium chloride–evoked dopamine release (K1, K2) in D2WT and D2KO mice. Graph on the right demonstrates dopamine concentration measured by the K2/K1 ratio in D2WT (1.05) and D2KO (1.38) mice (compared with D2WT, $^{*}p < .05$). GABA, gamma-aminobutyric acid; LMol, laconosum molecular layer; Ori, oriens; Pyr, pyramidal layer; Rad, stratum radiatum; TH, tyrosine hydroxylase.

mice resulted in a 1.4-fold increase in dopamine release compared with the first depolarization (K1), which was significantly higher than that observed in D2WT mice (1.16), implying the absence of inhibitory control from the presynaptic D2Rs on dopamine release (Figure 2F).

Constitutive Deletion of D2R Impaired Synaptic Plasticity in Temporal CA1

We examined whether remodeling of the VTA-hippocampus dopaminergic pathway in D2KO mice would impair NMDAR-dependent synaptic plasticity in CA1. In the dorsal area of temporal CA1, where DAT^+ fibers were detected, high-frequency stimulation induced significant LTP in hippocampus slices from D2WT mice ($n = 6$; 1.44 ± .06) but not in slices from D2KO mice ($n = 8$; 1.15 ± .07) (Figure 3A). For LTD expression, paired-pulse low-frequency stimulation induced stable depression in hippocampus slices from D2WT mice ($n = 9$; .83 ± .04) but not in slices from D2KO mice ($n = 7$; 1.08 ± .04) (Figure 3B). This reduction in long-term synaptic plasticity could be due to a change in glutamatergic transmission; in voltage clamp configuration, we recorded miniature excitatory postsynaptic currents in glutamatergic pyramidal neurons of temporal CA1 in D2KO ($n = 11$) and D2WT ($n = 11$) mice at −80 mV, in the presence of tetrodotoxin (Figure 3C). Neither the frequency (D2WT, .25 ± .02 Hz; D2KO, .28 ± .04 Hz) nor the amplitude (D2WT, 7.44 ± .42 pA; D2KO, 6.92 ± .49 pA) of the miniature excitatory postsynaptic currents was modified, suggesting that neither the glutamate spontaneous release nor the postsynaptic glutamate sensitivity was altered in CA3-CA1 synapses (Figure 3D). Paired-pulse facilitation of field excitatory postsynaptic potentials at CA3-CA1 glutamatergic synapses at increasing interpulse intervals was also conserved in D2KO brain slices (Figure 3E). However, field excitatory postsynaptic potentials recorded in the D2KO mice ($n = 10$) were significantly larger in the medium range than in D2WT mice ($n = 8$), revealing an increased excitability of CA3-CA1 synapses (Figure 3F). We wondered whether the increased dopamine released in D2KO mice would overactivate postsynaptic D_5 receptors expressed at CA1 glutamatergic cells and produce deficits in synaptic plasticity. The D_1/D_5 antagonist SCH23390 (1 μmol/L, 30 min) reinstated high-frequency stimulation–induced LTP on D2KO hippocampus slices to a level comparable to D2WT hippocampus slices ($n = 9$; 1.37 ± .06) (Figure 3G), whereas it had no effect on LTP induced in D2WT hippocampus slices ($n = 6$; 1.40 ± .09) (Figure S3A in Supplement 1). Nonetheless, SCH23390 application (1 μmol/L, 40 min) did not affect the level of LTD in D2KO hippocampus slices ($n = 6$; 1.04 ± .05) (Figure 3H).

Constitutive Deletion of D2R Caused Spatial and Recognition-Memory Deficits

In the spatial version of the MWM, D2KO mice were unable to learn the platform location. The mean latency during the last training session was significantly longer in D2KO mice (72.4 ± 7.4 sec) compared with D2WT mice (38.5 ± 8.9 sec). During the challenge session performed 90 min after the final training, D2KO mice (23% ± 4.7%) spent significantly less time in the active quadrant than D2WT mice (43.8% ± 2.2%), suggesting impairments in short-term spatial memory (Figure 4A). This deficit contrasted with the normal performance of D2KO mice in the cued version of the MWM (Figure 4B), where no differences in escape latencies were observed between the D2KO mice (day 5, 25.4 ± 5.4) and D2WT mice (day 5, 22.5 ± 5.4). In the spatial Barnes maze, D2KO mice acquired the escape hole location during training properly but did not significantly visit the active quadrant during the challenge session performed 24 hours after the last training (D2WT mice, 35.5 ± 4; D2KO mice, 21.6 ± 4.5), suggesting long-term spatial memory impairments (Figure 4C). Recognition memory was also impaired in the two-object recognition task; D2KO mice exhibited significantly decreased percentages of time spent exploring the new object compared with D2WT mice (D2KO mice, 53.1% ± 4%; D2WT mice, 65.2% ± 3.8%) (Figure 4D). Finally, D2KO mice exhibited no impairment in the fear-conditioning paradigm (Figure S4 in Supplement 1).

Pharmacologic Blockade of D2Rs Produced Loss of Spatial Memory and of Synaptic Plasticity in Hippocampus

Given the possible compensatory mechanisms that could occur during development in D2KO mice, we tested pharmacologic blockade of D2Rs in naïve C57BL/6J mice. Daily systemic administration of the D_2/D_3 receptor antagonist sulpiride (50 mg/kg) 30 min before the first of two training sessions in the spatial version of the MWM revealed a slow-onset effect. During the first 4 training days, the escape latencies in the sulpiride group (58.3 ± 11 sec) and the sodium chloride group (50.3 ± 5.4 sec) were identical. However, during subsequent training sessions, sulpiride-treated mice were slower to find the platform location (sulpiride group, 70.2 ± 10.6 sec; control group, 39.6 ± 7.3 sec), and spent less time in the active quadrant (sulpiride group, 21.1% ± 10.4%; control group, 42.6% ± 4.1%) during the challenge (Figure 5A). When sulpiride treatment started 1 week before the MWM training and was maintained during the procedure, the mice were unable to learn the platform location (sulpiride group, 71.1 ± 9.5 sec; control group, 44.1 ± 10.1 sec) and spent significantly less time in the active quadrant during the challenge (sulpiride group, 17.5% ± 3.7%; control group, 42.6% ± 4.1%) (Figure 5B). If the sulpiride pretreatment was stopped before the MWM training, the deficit during the first 3 days of training (sulpiride group, 80.4 ± 5.9 sec; control group, 60 ± 4.6 sec) disappeared during the last days (sulpiride group, 44.1 ± 10.1 sec; control group, 39.6 ± 7.3 sec) and during the challenge (sulpiride group, 36% ± 4.9%; control group, 42.6% ± 4.1%) (Figure 5C).

To assess the acute effects of D2R blockade on synaptic plasticity, we applied sulpiride (10 μmol/L) to C57BL/6J hippocampus slices during LTP and LTD induction. Application of sulpiride produced the same impairment pattern observed in D2KO hippocampus slices. Both LTP ($n = 7$; 1.55 ± .1) and LTD ($n = 7$; .78 ± .08) were observed in the untreated slices, whereas sulpiride produced a significant decrease in LTP ($n = 8$; 1.30 ± .06) (Figure 5D) and abolition of LTD expression ($n = 6$; 1.03 ± .05) (Figure 5E).

As in D2KO mice, C57Bl/6J mice treated for 15 days with sulpiride demonstrated a highly significant sprouting (1.3-fold

to 1.7-fold more) of DAT^{+} fibers in laconosum moleculare layer (sulpiride group, 132.3 ± 22.5; control group, 99.1 ± 10.6), radiatum (sulpiride group, 126.7 ± 5.9; control group, 76.2 ± 5.9), and pyramidal layer and oriens (sulpiride group, 51.1 ± 6.4; control group, 32.7 ± 2.2) layers (Figure 5F; Figure S2H,H′ in Supplement 1). Dopamine levels were also increased in treated mice (sulpiride group, 204.4 ± 20.1 ng/g; control group, 169.8 ± 12.4 ng/g), attesting to the fast remodeling of the dopamine system in the hippocampus (Figure 5G; Figure S2I in Supplement 1).

To confirm the association of the effects of D2R blockade with hippocampal-dependent processes, we implanted bilateral cannulas into the temporal part of the hippocampi of C57BL/6J mice (Figure S2J in Supplement 1). Direct sulpiride

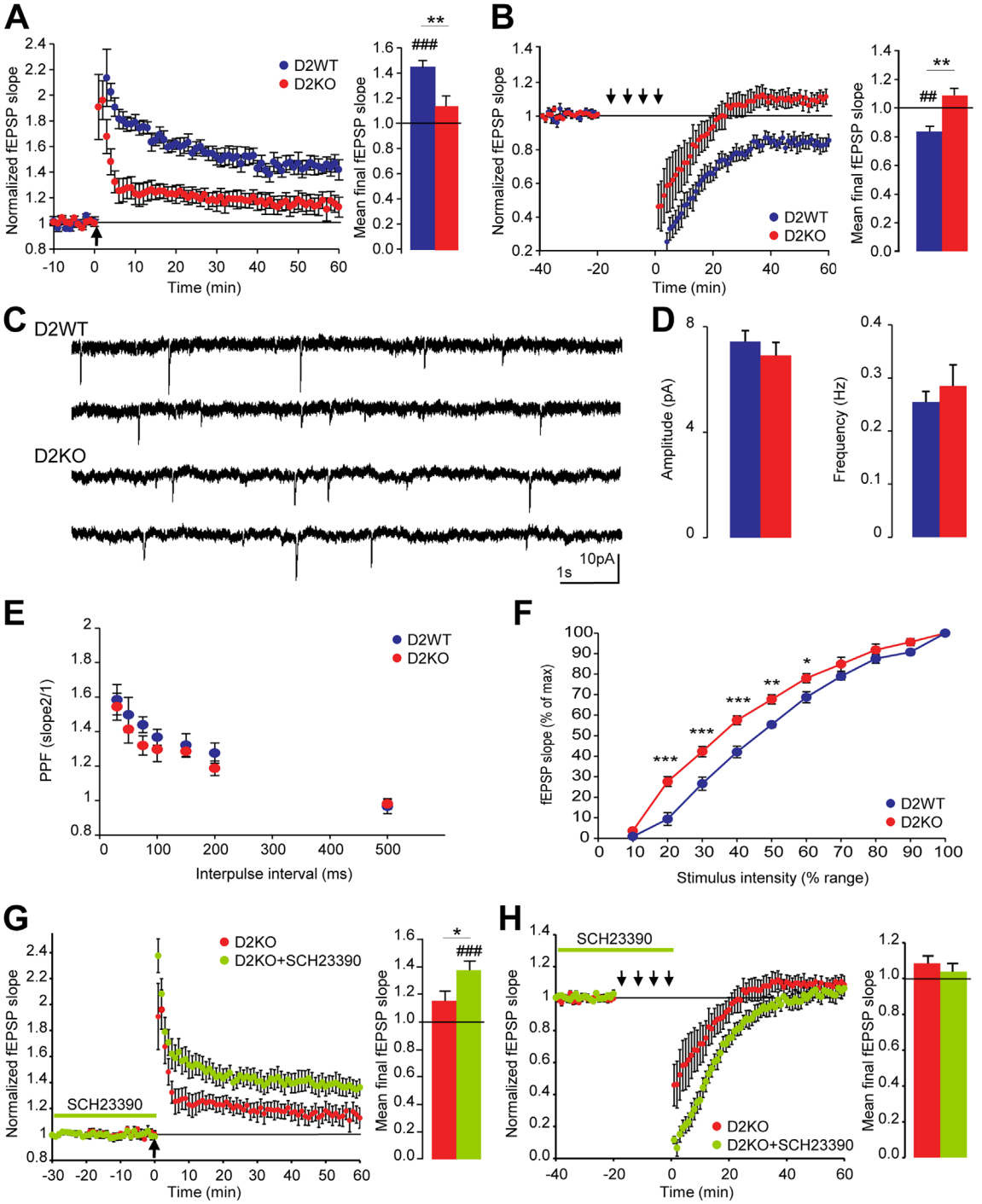

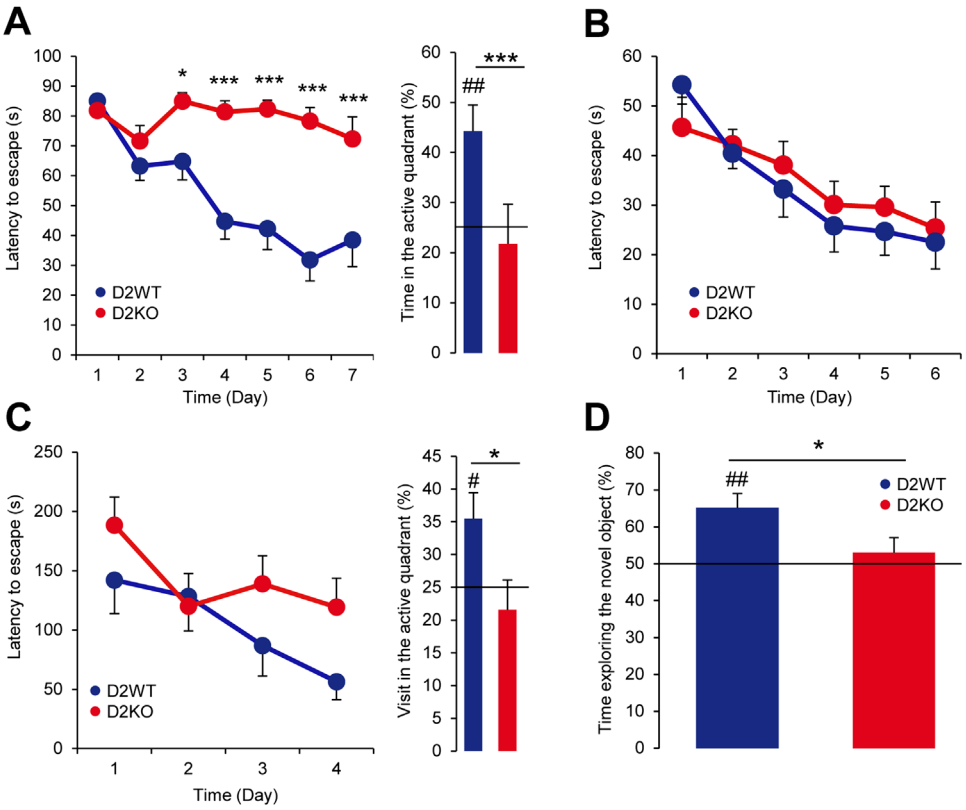

Figure 4. Hippocampal-dependent memory performance in D_2 knockout (D2KO) mice. **(A)** Graph on the left demonstrates mean escape latency in the spatial hidden-platform version of the Morris water maze in D_2 wild-type (D2WT) ($n = 17$) and D2KO ($n = 18$) mice (compared with D2WT, $^{*}p < .05$, $^{***}p < .001$). Graph on the right demonstrates percentage of time spent in the active quadrant during the probe test of the Morris water maze in each genotype (compared with chance performance of 25%, $^{\#\#}p < .01$; compared with D2WT, $^{*}p < .05$). **(B)** Mean escape latency in the cued version of the Morris water maze for D2WT ($n = 16$) and D2KO ($n = 15$) mice. **(C)** Graph on the left demonstrates escape latency in the spatial Barnes maze in D2WT ($n = 9$) and D2KO ($n = 10$) mice. Graph on the right demonstrates percentage of time spent in the active quadrant during the probe test of the Barnes maze in each genotype (compared with chance performance of 25%, $^{\#}p < .05$; compared with D2WT, $^{*}p < .05$). **(D)** Percentage of time exploring the new object in the novel object recognition task in D2WT ($n = 9$) and D2KO ($n = 10$) mice (compared with chance performance of 50%, $^{\#\#}p < .01$; compared with D2WT, $^{*}p < .05$).

infusion (5 μg/μL, .1 μL/side), initiated 1 week before the MWM procedure and maintained during training, reproduced the learning deficit observed in D2KO mice (Figure 5H). The final escape latency was significantly increased in sulpiride-treated mice (77.3 ± 6.6 sec) compared with control mice (29 ± 7.5 sec), and the time spent in the active quadrant was significantly decreased (19.6% ± 3.9%) compared with controls (33.2% ± 4.1%).

D2R Deletion in DAT^{+} Neurons Was Sufficient to Impair LTD Expression and Spatial Memory Formation in Hippocampus

To assess specifically the contribution of presynaptic D2Rs, we crossed *Drd2*$^{loxP/loxP}$ mice (36) with BAC-DATicre mice (37) to remove D_2 autoreceptors in DAT^{+} neurons (Figure S5A–C in Supplement 1). Presynaptic knockout of the D2R gene (D2^{DATcre} mice) had no effect on the expression of LTP in CA1 ($n = 8$; 1.40 ± .05) compared with WT^{DATcre} mice ($n = 6$; 1.44 ± .06) (Figure 6A). Conversely, D2^{DATcre} mice totally lost LTD expression ($n = 6$; 1.06 ± .05) compared with WT^{DATcre} mice ($n = 9$; .83 ± .04) (Figure 6B). The input-output relationship in evoked glutamatergic field excitatory postsynaptic potentials was not different between the D2^{DATcre} mice and their WT^{DATcre} littermates (Figure 6C). To assess whether this LTD deficit could be a consequence of presynaptic D2R absence on dopamine release and synthesis, we analyzed DAT^{+} fiber density and dopamine tissue levels in the temporal hippocampus of D2^{DATcre} mice. We found that D2^{DATcre} mice

Figure 3. Synaptic plasticity of the temporal hippocampus in D_2 knockout (D2KO) mice. **(A)** Graph on the left demonstrates high-frequency stimulation–induced long-term potentiation in D_2 wild-type (D2WT) ($n = 6$) and D2KO ($n = 8$) hippocampus slices. Graph on the right demonstrates mean final slope in each genotype (compared with baseline, $^{\#\#\#}p < .001$; compared with D2WT, $^{**}p < .01$). **(B)** Graph on the left demonstrates paired-pulse low-frequency stimulation–induced long-term depression in D2WT ($n = 9$) and D2KO ($n = 7$) hippocampus slices. Graph on the right demonstrates mean final slope in each genotype (compared with baseline, $^{\#\#}p < .01$; compared with D2WT, $^{**}p < .01$). **(C)** Examples of traces of miniature excitatory postsynaptic currents recorded in CA1 pyramidal cells of D2WT and D2KO hippocampus slices at −80 mV. **(D)** Mean amplitude and frequency of miniature excitatory postsynaptic currents recorded in D2WT and D2KO hippocampus slices ($n = 11$ cells in each group). **(E)** Paired-pulses facilitation (PPF) in D2WT ($n = 7$; 30 msec, 1.58 ± .09; 50 msec, 1.50 ± .10; 75 msec, 1.44 ± .05; 100 msec, 1.37 ± .05; 150 msec, 1.32 ± .07; 200 msec, 1.27 ± .06; 500 msec, .97 ± .04) and D2KO ($n = 7$; 30 msec, 1.54 ± .08; 50 msec, 1.41 ± .08; 75 msec, 1.32 ± .06; 100 msec, 1.30 ± .07; 150 msec, 1.28 ± .03; 200 msec, 1.18 ± .04; 500 msec, .98 ± .03) hippocampus slices. **(F)** Input-output relationship at CA3-CA1 synapses in D2WT ($n = 8$) and D2KO ($n = 10$) hippocampus slices (compared with D2WT, $^{***}p < .001$, $^{**}p < .01$, $^{*}p < .05$). Each recorded fEPSP was normalized by the fEPSP recorded for the maximum intensity of stimulation. **(G)** Graph on the left demonstrates high-frequency stimulation–induced long-term potentiation in D2KO hippocampus slices after SCH23390 (1 μmol/L, 30 min) application ($n = 9$) compared with untreated D2KO slices ($n = 8$). Graph on the right demonstrates mean final slope in each condition (compared with baseline, $^{\#\#\#}p < .001$; compared with untreated slices, $^{*}p < .05$). **(H)** Graph on the left demonstrates paired-pulse low-frequency stimulation–induced long-term depression in D2KO hippocampus slices after SCH23390 (1 μmol/L, 40 min) application ($n = 6$) compared with untreated D2KO slices ($n = 7$). Graph on the right demonstrates mean final slope in each condition (no significant difference). fEPSP, field excitatory postsynaptic potential.

exhibited 3.3-fold and 7.5-fold more DAT^{+} fibers in the radiatum ($D2^{DATcre}$, 228.3 ± 55.6; WT^{DATcre}, 68.4 ± 12.5) and in the oriens and pyramidal cell layers ($D2^{DATcre}$, 221.8 ± 64.9; WT^{DATcre}, 29.4 ± 15.3), respectively, compared with WT^{DATcre} littermates, with no changes in the laconosum moleculare layer ($D2^{DATcre}$, 81.5 ± 17.3; WT^{DATcre}, 89.2 ± 33.9) (Figure 6E). Finally, we observed a significant 1.3-fold increase in tissue dopamine levels in the temporal hippocampus of the $D2^{DATcre}$ mice compared with WT^{DATcre} mice (Figure 6F; Figure S5E in Supplement 1).

The $D2^{DATcre}$ mice exhibited dramatic memory impairments in the spatial version of the MWM. The final mean escape latency was significantly increased in the $D2^{DATcre}$ mice (50.9 ± 11.2 sec) compared with WT^{DATcre} mice (21.8 ± 8.8 sec), and the percentage of time spent in the active quadrant was significantly decreased in $D2^{DATcre}$ mice (22.4% ± 6.7%) compared with WT^{DATcre} mice (44.2% ± 3.9%) (Figure 6G). Further linking the role of LTD in these memory deficits, although blockade of D1Rs with SCH23390 rescued high-frequency stimulation–induced LTP expression in D2KO hippocampus slices, it had no effect on LTD deficits or on memory deficits (Figure 3H; Figure S3B in Supplement 1).

DISCUSSION

Organization of Dopamine Circuitry in Hippocampus Suggests Tonic Functional Mode of Transmission

We localized dopamine receptor–expressing cells using sensitive in situ hybridization techniques; D_5 dopamine receptor mRNA expression in the entire granular cell layer of the DG and the pyramidal cell layer of CA1 and CA3 as well as D1R expression

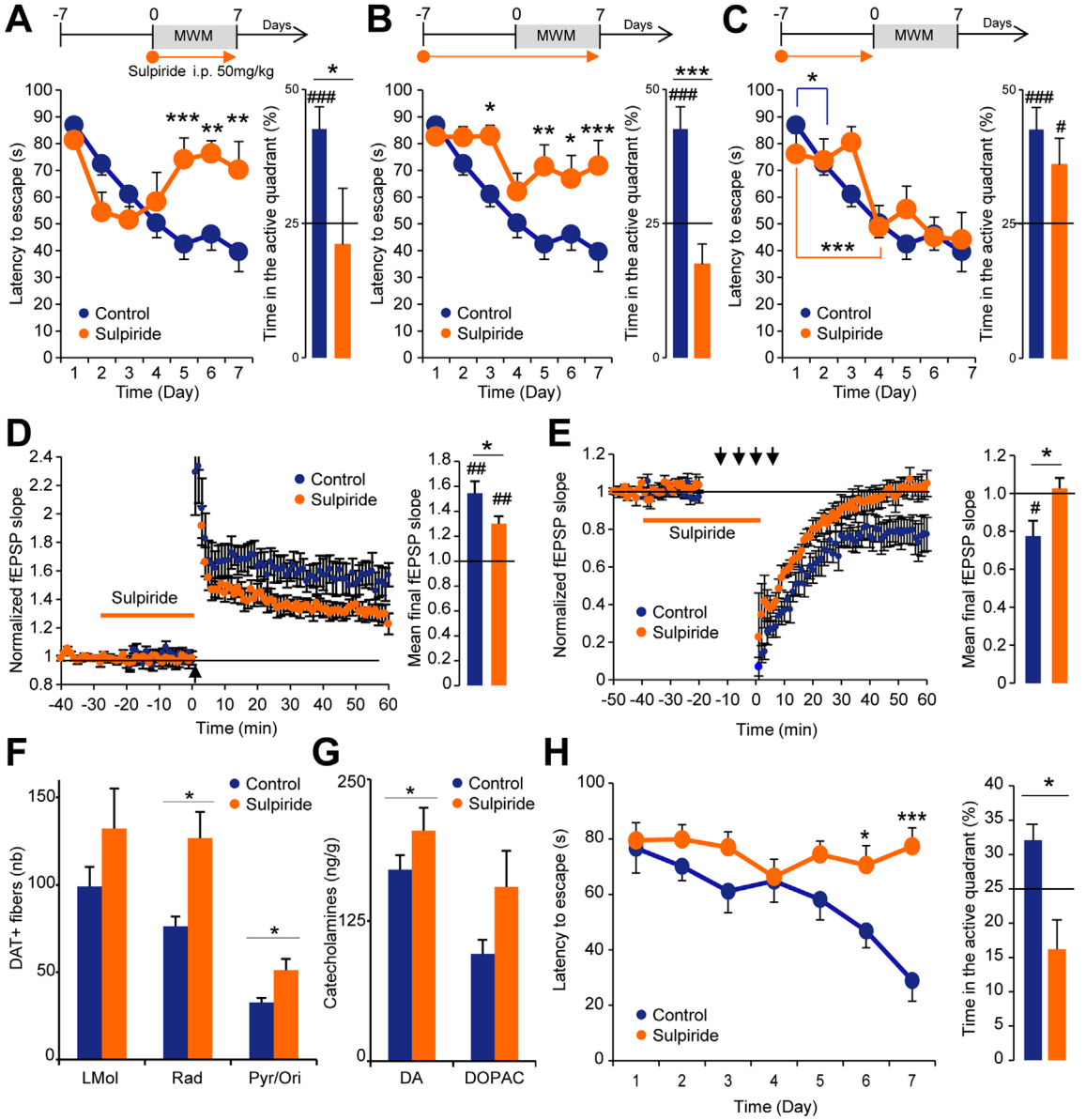

restricted to the granular cells of the DG confirm previous reports in rats and primates (39–43). We could not detect D_3 dopamine receptor or D_4 dopamine receptor transcript expression in the hippocampus: D_3 dopamine mRNA was observed only in the amygdalohippocampal area (44), but the absence of D_4 dopamine mRNA contrasts with its previously described participation in CA1 synapses depotentiation through CA3 GABAergic interneurons (45,46). The restricted expression of D2R in the hilus as well as in the DG flanking the granular cell layer was shown in mRNA localization and binding experiments. Because D2R binding was detectable in the hippocampus of $D2^{DATcre}$ mice (Figure S5D in Supplement 1), it clearly indicated that the labeling in the DG mostly originated from the hilar D2-positive cells. The demonstration that D_2 dopamine mRNA colocalized with CaMK2α in the hilus confirmed the report of putative D2R expression in mossy cells using Drd2-EGFP transgenic mice (47). Morphologic characteristics of these cells confirmed that these were glutamate mossy interneurons (48–50).

Dopaminergic innervation, assessed by DAT expression, was restricted to the temporal area of CA1. The organization of the dopamine system, with an absence of DAT^+ fibers in the polymorphic layers of the DG, is typical of a volume transmission modus operandi (51–53). Retrograde labeling with RetroBeads injected into the temporal hippocampus confirmed results obtained in rats (54); we showed ~20% of the efferent VTA neurons are TH-positive neurons and identified all other projecting neurons as GABAergic. Using in vivo microdialysis, we showed that the functionally releasable pool of dopamine is under the control of presynaptic D2 activation, as described in the striatum (35,36). The presynaptic D2Rs conferred to dopamine neurons a high structural plasticity, as shown by the massive sprouting of DAT^+ fibers in the D2KO, $D2^{DATcre}$ mice and following long-term treatment with sulpiride. This observation is in accordance with previous studies reporting that D2R activation exerted an inhibitory effect on dopamine sprouting in the striatum (55,56). The upregulation of DAT fibers, dopamine tissue, and dopamine release levels suggests that long-term use of antipsychotics could produce drastic anatomic changes in the hippocampus.

Dopamine D2Rs Control Plasticity of Temporal Hippocampus

The potential role played by D2Rs in the modulation of long-term hippocampal synaptic plasticity has been poorly documented (21,25). Our anatomic description emphasized a critical role for presynaptic D2Rs in DAT fiber architecture in the temporal region. We focused on this region to investigate the role of D2R activation in synaptic plasticity.

In D2KO mice, we observed a suppression of both LTP and LTD after high-frequency stimulation or paired-pulse low-frequency stimulation of the Schaffer collaterals in temporal CA1. As was previously reported regarding corticostriatal plasticity (57), no critical changes in basal glutamatergic transmission were detected. Because we could not detect postsynaptic D2R expression in CA1, we assumed that D_5 dopamine receptor overactivation at glutamatergic cells was potentially involved. Blocking D1Rs with SCH23390 in D2KO hippocampus slices reestablished LTP levels but did not restore LTD. Functional response of D1R activation has been shown to follow an inverted U–shaped curve in the prefrontal cortex (58). Our results suggested that this model is relevant regarding LTP expression at glutamatergic synapses of CA1, but that LTD expression responds to different mechanisms.

The impairments in LTP and LTD were almost entirely replicated by application in C57BL/6J mice slices of sulpiride, which has high specificity for D_2/D_3 receptors (59). In particular, LTD was fully blocked as reported in D2KO mice. These results showed that D2Rs played a pivotal role in the expression of CA3-CA1 plasticity.

Dopamine D2Rs Control Spatial Learning in Temporal Hippocampus

Given the drastic changes in synaptic plasticity and the dopaminergic circuit remodeling observed in D2KO and sulpiride-treated mice, we anticipated downstream functional impairments in hippocampus-dependent learning and memory processes. Systemic administration of D_2-like antagonists in rats had been

Figure 5. Spatial memory performance and synaptic plasticity after pharmacologic blockage of D_2 receptors by sulpiride. **(A)** Graph on the left demonstrates mean escape latency in the spatial hidden-platform version of the Morris water maze (MWM) in control (sodium chloride [NaCl] .9%, $n = 21$) and sulpiride-treated (intraperitoneal injection 50 mg/kg, $n = 9$) mice during the 7 days of the MWM (compared with control mice, $^*p < .05$, $^{**}p < .01$, $^{***}p < .001$). Graph on the right demonstrates percentage of time spent in the active quadrant during the probe test of the MWM in each condition (compared with chance performance of 25%, $^{###}p < .001$; compared with control mice, $^*p < .05$). **(B)** Graph on the left demonstrates mean escape latency in the spatial hidden-platform version of the MWM in control (NaCl .9%, $n = 21$) and sulpiride-treated (intraperitoneal injection 50 mg/kg, $n = 11$) mice with treatment started 7 days before the MWM and continued during the 7 days of the experiment (compared with control mice, $^*p < .05$, $^{**}p < .01$, $^{***}p < .001$). Graph on the right demonstrates percentage of time spent in the active quadrant during the probe test of the MWM in each condition (compared with chance performance of 25%, $^{###}p < .001$; compared with control mice, $^{***}p < .001$). **(C)** Graph on the left demonstrates mean escape latency in the spatial hidden-platform version of the MWM in control (NaCl .9%, $n = 21$) and sulpiride-treated (intraperitoneal injection 50 mg/kg, $n = 11$) mice with treatment started 7 days before the MWM but stopped during the 7 days of the experiment (compared with day 1, $^*p < .05$, $^{***}p < .001$). Graph on the right demonstrates percentage of time spent in the active quadrant during the probe test of the MWM in each condition (compared with chance performance of 25%, $^{\#}p < .05$, $^{###}p < .001$). **(D)** Graph on the left demonstrates high-frequency stimulation–induced long-term potentiation in C57BL/6J hippocampus slices after sulpiride (10 μmol/L, 30 min) application ($n = 9$) compared with untreated slices ($n = 7$). Graph on the right demonstrates mean of the final slope in each condition (compared with baseline, $^{\#\#}p < .01$; compared with untreated slices, $^*p < .05$). **(E)** Graph on the left demonstrates paired-pulse low-frequency stimulation–induced long-term depression in C57BL/6J hippocampus slices after sulpiride (10 μmol/L, 40 min) application ($n = 6$) compared with untreated slices ($n = 8$). Graph on the right demonstrates mean of the final slope in each condition (compared with baseline, $^{\#}p < .05$; compared with untreated slices, $^*p < .05$). **(F)** Quantification of dopamine transporter–positive (DAT^+) fiber immunostaining in CA1 layers of the right hippocampus in control and sulpiride-treated mice ($n = 4$ for each group; compared with wild-type mice, $^*p < .05$). **(G)** High-pressure liquid chromatography analysis of tissue catecholamine (dopamine [DA] and 3,4-dihydroxyphenylacetic acid [DOPAC]) levels in the hippocampus of control ($n = 7$) and sulpiride-treated ($n = 7$) mice (compared with control, $^*p < .05$). **(H)** Graph on the left demonstrates mean escape latency in the spatial hidden-platform version of the MWM for control (NaCl .9%; $n = 10$) and sulpiride-treated (2.5 μg injected each side; $n = 11$) mice (compared with control mice, $^*p < .05$, $^{***}p < .005$). Graph on the right demonstrates percentage of time spent in the active quadrant during the probe test of the MWM in each condition (compared with control mice, $^*p < .05$). fEPSP, field excitatory postsynaptic potential; LMol, laconosum molecular layer; Ori, oriens; Pyr, pyramidal layer; Rad, stratum radiatum.

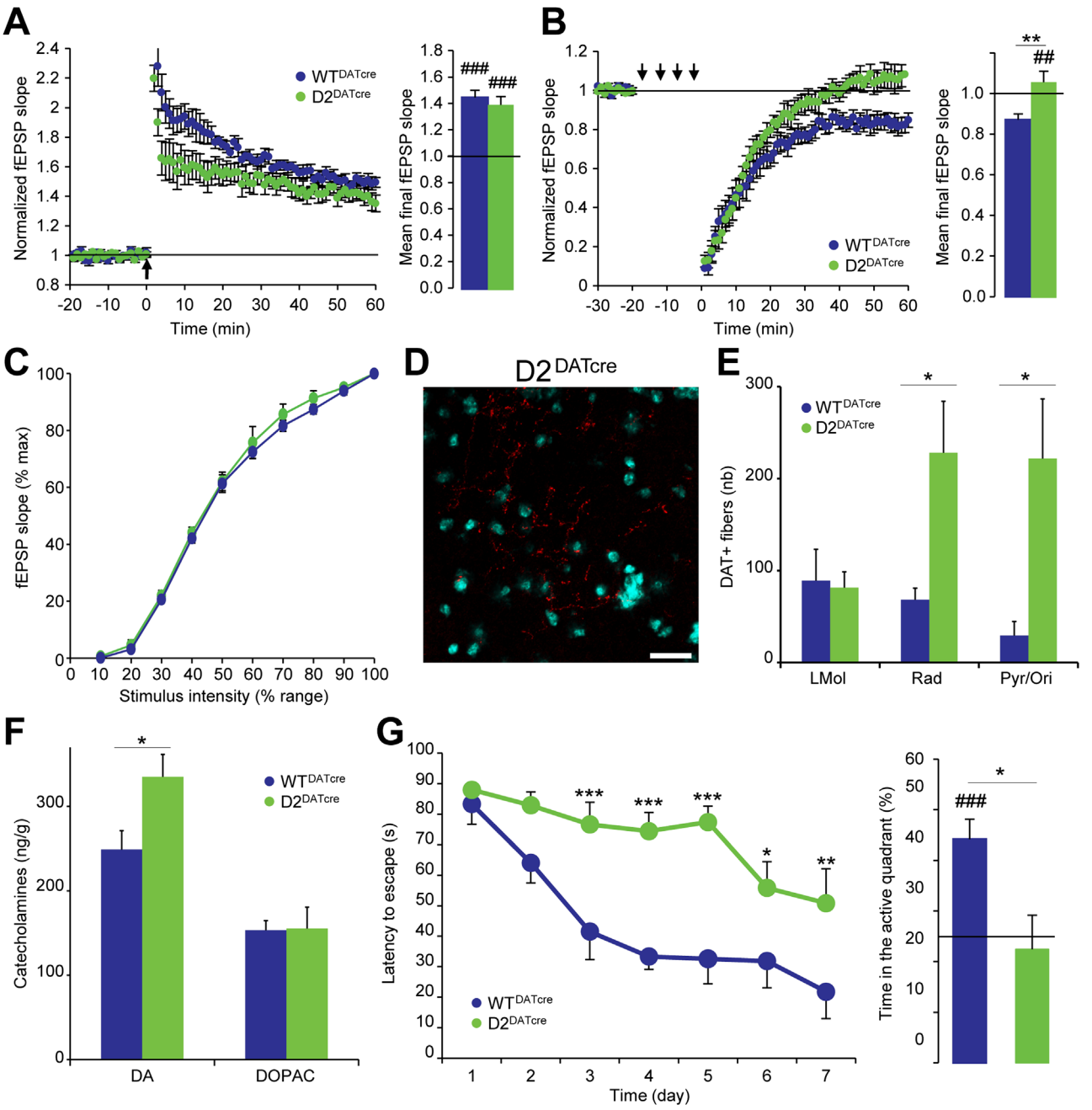

Figure 6. Synaptic plasticity, anatomic characterization, and spatial memory in presynaptic D_2 receptor knockout mice. **(A)** Graph on the left demonstrates high-frequency stimulation–induced long-term potentiation in WT^{DATCre} ($n = 6$) and $D2^{DATCre}$ ($n = 9$) hippocampus slices. Graph on the right demonstrates mean of the final slope in each genotype (compared with baseline, $^{###}p < .001$). **(B)** Graph on the left demonstrates paired-pulse low-frequency stimulation–induced long-term depression in WT^{DATCre} ($n = 7$) and $D2^{DATCre}$ ($n = 6$) hippocampus slices. Graph on the right demonstrates mean of the final slope in each genotype (compared with baseline, $^{##}p < .01$; compared with WT^{DATCre}, $^{**}p < .01$). **(C)** Intensity-amplitude (input-output) relationship at CA3-CA1 synapses in WT^{DATCre} ($n = 7$) and $D2^{DATCre}$ ($n = 6$) hippocampus slices. Each recorded fEPSP was normalized by the fEPSP recorded for the maximum intensity of stimulation. **(D)** Image of dopamine transporter–positive (DAT^+) fibers in the stratum radiatum layer of the CA1 temporal hippocampus in $D2^{DATCre}$ mice. (Scale bar = 50 μm.) **(E)** Quantification of DAT^+ fiber immunostaining in CA1 layers of the right hippocampus in WT^{DATCre} and $D2^{DATCre}$ mice ($n = 4$ for each group; compared with WT^{DATCre}, $^{*}p < .05$). **(F)** High-pressure liquid chromatography analysis of tissue catecholamine (dopamine [DA] and 3,4-dihydroxyphenylacetic acid [DOPAC]) levels in the hippocampus of WT^{DATCre} ($n = 7$) and $D2^{DATCre}$ ($n = 8$) mice (compared with WT^{DATCre}, $^{*}p < .05$). **(G)** Graph on the left demonstrates mean escape latency in the spatial hidden-platform version of the Morris water maze in WT^{DATCre} ($n = 9$) and $D2^{DATCre}$ ($n = 10$) mice (compared with WT^{DATCre}, $^{*}p < .05$, $^{**}p < .01$, $^{***}p < .005$). Graph on the right demonstrates percentage of time spent in the active quadrant during the probe test of the Morris water maze in each genotype (compared with chance performance of 25%, $^{###}p < .001$; compared with WT^{DATCre}, $^{*}p < .05$). fEPSP, field excitatory postsynaptic potential; LMol, laconosum molecular layer; Ori, oriens; Pyr, pyramidal layer; Rad, stratum radiatum.

shown to trigger learning and memory deficits (28,30,32,60–62). The profound deficits in both LTP and LTD observed in D2KO mice were associated with dramatic impairments in three hippocampus-dependent learning and memory paradigms: the spatial MWM, the Barnes maze, and the novel object recognition task. The absence of deficits in the cued version of the MWM, known to involve mainly striatal dopamine regulation (63,64), implied an absence of sensorimotor deficits in the D2KO strain.

The experiments using various treatment times with sulpiride provided greater insight into the rapid dynamics of changes that occur after D2R blockade and revealed a reversible adaptive response controlled by D2R activity. This observation is consistent with the rapid onset of the beneficial effects of antipsychotics on positive symptoms of schizophrenia in human patients (65). Finally, stereotactic administration of sulpiride into the temporal hippocampi of C57BL/6J mice fully replicated the learning deficit observed in D2KO mice. This finding unambiguously demonstrated the specific participation of D2Rs localized in the temporal hippocampus in the performance of the MWM.

Specific Deletion of Presynaptic D2Rs Is Correlated with LTD Absence in Temporal Hippocampus and Learning Deficits

In $D2^{DATcre}$ mice, with presynaptic D2R deletion, a dichotomy between LTP and LTD expression was observed—LTP expression remained intact, whereas LTD was abolished. Performance in the spatial MWM was equally impaired in $D2^{DATcre}$ and in D2KO mice. Different molecular mechanisms, with potentially distinct roles, are responsible for the operation of LTP and LTD (66,67). In particular, LTD has been shown to be essential for spatial memory consolidation (68), novel spatial learning (69), and behavioral flexibility (70). The expression of NMDAR-dependent LTD in the hippocampus relies on phosphatase activity (71), whereas the expression of NMDAR-dependent LTP relies on the postsynaptic activation of calcium/calmodulin–dependent kinase II and trafficking of GluA1-containing α-amino-3-hydroxy-5-methyl-4-isoxazole-propionic acid receptors (72). The activity of the G protein–independent glycogen synthase kinase 3beta/Akt pathway might be required in NMDAR-dependent LTD expression in the hippocampus (73,74). In the mouse striatum, D2R activation is essential for Akt inhibition and glycogen synthase kinase 3beta activation (7,75); the recruitment of these pathways in D_2 dopamine–dependent plasticity in the hippocampus remains to be investigated.

Another question is the function of D2Rs expressed in the mossy cells of the DG. Although it is unlikely that these postsynaptic D2Rs would be implicated in LTD and spatial memory deficits, because they are intact in $D2^{DATcre}$ mice, they might participate in the deficit of LTP expression of D2KO mice through a modulation of CA3 to CA1 excitability.

In conclusion, our data reveal that LTD expression in the temporal hippocampus plays a determinant role in the regulation of learning and memory and that presynaptically expressed D2Rs in dopamine fibers tightly modulate this aspect of hippocampus function. On the one hand, D2Rs control synaptic and extrasynaptic dopamine levels, dopamine innervation, LTD expression thresholds, and learning and memory performance through their presynaptic location in temporal CA1. On the other hand, D2Rs seem to be implicated in LTP modulation through postsynaptic D1R overactivation. Even if a clarification of the mechanisms involved in these processes is still necessary, these contributions were largely underestimated until now. The functional role of VTA dopaminergic input in the hippocampus potentially shapes a complex circuitry when added to the loop from the hippocampus to the nucleus accumbens and then to the VTA, which has been shown to control the firing of dopamine neurons (10,76). The existence of a direct mesohippocampal functional dopamine pathway and the role of presynaptic D2Rs are key elements to consider in the etiology of psychotic symptoms and the long-term effects of antipsychotic treatments, including their potential impact on hippocampal volume in patients with schizophrenia (77) and the role of dopamine in aberrant salience and the etiology of delusions (78).

ACKNOWLEDGMENTS AND DISCLOSURES

This work was supported by the Canada Research Chairs program (BG is a Canadian Research Chair in the Neurobiology of Mental Disorders), the Canadian Foundation for Innovation, the Graham Boeckh Foundation for Schizophrenia Research (BG), and the Fond de Recherche du Québec-Santé (postdoctorate grants to GDB and EI). We thank Erika Vigneault and Marie-Eve Desaulnier for excellent care and maintenance of all mice colonies.

The authors report no biomedical financial interests or potential conflicts of interest.

ARTICLE INFORMATION

Department of Psychiatry (JR, EI, GDB, SS, AM, LM, AG, TPW, BG), Douglas Mental Health University Institute, McGill University, Montreal, Quebec, Canada; Institut national de la santé et de la recherche médicale (FT, BG), Unité Mixte de Recherche en Santé 1130, and Centre National de la Recherche Scientifique, Unité Mixte de Recherche 8246, Sorbonne University Université Pierre et Marie Curie, Neuroscience Paris Seine, Paris, France; Département de Pharmacie (DL), Université de Montréal, Montreal, Quebec, Canada; Instituto de Investigaciones en Ingeniería Genética y Biología Molecular, Instituto de Investigaciones en Ingenieria Genética y Biologia Molecular (CONICET), Biología Molecular y Celular, Facultad de Ciencias Exactas y Naturales, Universidad de Buenos Aires, Argentina; and Departamento de Fisiología (MR), Biología Molecular y Celular, Facultad de Ciencias Exactas y Naturales, Universidad de Buenos Aires, Argentina.

Authors JR, EI, and GDB contributed equally to this work.

Address correspondence to Bruno Giros, Ph.D., Department of Psychiatry, Douglas Mental Health University Institute, 6875 Lasalle Boulevard, McGill University, Montreal, Quebec, H4H 1R3, Canada; E-mail: bruno.giros@mcgill.ca

Received Jan 22, 2014; revised Mar 4, 2014; accepted Mar 13, 2014.

Supplementary material cited in this article is available online at http://dx.doi.org/10.1016/j.biopsych.2014.03.013.

REFERENCES

1. Beninger RJ (1983): The role of dopamine in locomotor activity and learning. Brain Res 287:173–196.
2. Wise RA, Rompre PP (1989): Brain dopamine and reward. Annu Rev Psychol 40:191–225.
3. Cools R (2006): Dopaminergic modulation of cognitive function-implications for L-DOPA treatment in Parkinson's disease. Neurosci Biobehav Rev 30:1–23.
4. Nieoullon A (2002): Dopamine and the regulation of cognition and attention. Prog Neurobiol 67:53–83.
5. Weinberger DR, Berman KF, Chase TN (1988): Mesocortical dopaminergic function and human cognition. Ann N Y Acad Sci 537:330–338.

6. Tritsch NX, Sabatini BL (2012): Dopaminergic modulation of synaptic transmission in cortex and striatum. Neuron 76:33–50.
7. Beaulieu JM, Del'guidice T, Sotnikova TD, Lemasson M, Gainetdinov RR (2011): Beyond cAMP: The regulation of Akt and GSK3 by dopamine receptors. Front Mol Neurosci 4:38.
8. Gasbarri A, Sulli A, Packard MG (1997): The dopaminergic mesencephalic projections to the hippocampal formation in the rat. Prog Neuropsychopharmacol Biol Psychiatry 21:1–22.
9. Swanson LW (1982): The projections of the ventral tegmental area and adjacent regions: A combined fluorescent retrograde tracer and immunofluorescence study in the rat. Brain Res Bull 9:321–353.
10. Lisman JE, Pi HJ, Zhang Y, Otmakhova NA (2010): A thalamo-hippocampal-ventral tegmental area loop may produce the positive feedback that underlies the psychotic break in schizophrenia. Biol Psychiatry 68:17–24.
11. Boyer P, Phillips JL, Rousseau FL, Ilivitsky S (2007): Hippocampal abnormalities and memory deficits: New evidence of a strong pathophysiological link in schizophrenia. Brain Res Rev 54:92–112.
12. Folley BS, Astur R, Jagannathan K, Calhoun VD, Pearlson GD (2010): Anomalous neural circuit function in schizophrenia during a virtual Morris water task. Neuroimage 49:3373–3384.
13. Hanlon FM, Weisend MP, Hamilton DA, Jones AP, Thoma RJ, Huang M, *et al*. (2006): Impairment on the hippocampal-dependent virtual Morris water task in schizophrenia. Schizophr Res 87:67–80.
14. Ledoux A-A, Phillips JL, Labelle A, Smith A, Bohbot VD, Boyer P (2013): Decreased fMRI activity in the hippocampus of patients with schizophrenia compared to healthy control participants, tested on a wayfinding task in a virtual town. Psy Res Neuroimaging 211:47–56.
15. Biscoe TJ, Straughan DW (1966): Micro-electrophoretic studies of neurones in the cat hippocampus. J Physiol 183:341–359.
16. Beaulieu JM, Gainetdinov RR (2011): The physiology, signaling, and pharmacology of dopamine receptors. Pharmacol Rev 63:182–217.
17. Jay TM (2003): Dopamine: a potential substrate for synaptic plasticity and memory mechanisms. Prog Neurobiol 69:375–390.
18. Frey U, Matthies H, Reymann KG, Matthies H (1991): The effect of dopaminergic D1 receptor blockade during tetanization on the expression of long-term potentiation in the rat CA1 region in vitro. Neurosci Lett 129:111–114.
19. Lemon N, Manahan-Vaughan D (2006): Dopamine D1/D5 receptors gate the acquisition of novel information through hippocampal long-term potentiation and long-term depression. J Neurosci 26: 7723–7729.
20. Lisman J, Grace AA, Duzel E (2011): A neoHebbian framework for episodic memory: Role of dopamine-dependent late LTP. Trends Neurosci 34:536–547.
21. Huang YY, Kandel ER (1995): D1/D5 receptor agonists induce a protein synthesis-dependent late potentiation in the CA1 region of the hippocampus. Proc Natl Acad Sci U S A 92:2446–2450.
22. Otmakhova NA, Lisman JE (1996): D1/D5 dopamine receptor activation increases the magnitude of early long-term potentiation at CA1 hippocampal synapses. J Neurosci 16:7478–7486.
23. Matthies H, Becker A, Schroeder H, Kraus J, Hollt V, Krug M (1997): Dopamine D1-deficient mutant mice do not express the late phase of hippocampal long-term potentiation. Neuroreport 8:3533–3535.
24. El-Ghundi M, Fletcher PJ, Drago J, Sibley DR, O'Dowd BF, George SR (1999): Spatial learning deficit in dopamine D(1) receptor knockout mice. Eur J Pharmacol 383:95–106.
25. Chen Z, Ito K, Fujii S, Miura M, Furuse H, Sasaki H, *et al*. (1996): Roles of dopamine receptors in long-term depression: Enhancement via D1 receptors and inhibition via D2 receptors. Receptors Channels 4:1–8.
26. Packard MG, White NM (1991): Dissociation of hippocampus and caudate nucleus memory systems by posttraining intracerebral injection of dopamine agonists. Behav Neurosci 105:295–306.
27. Wilkerson A, Levin ED (1999): Ventral hippocampal dopamine D1 and D2 systems and spatial working memory in rats. Neuroscience 89: 743–749.
28. Terry AV Jr, Hill WD, Parikh V, Evans DR, Waller JL, Mahadik SP (2002): Differential effects of chronic haloperidol and olanzapine exposure on brain cholinergic markers and spatial learning in rats. Psychopharmacology (Berl) 164:360–368.
29. Terry AV Jr, Parikh V, Gearhart DA, Pillai A, Hohnadel E, Warner S, *et al*. (2006): Time-dependent effects of haloperidol and ziprasidone on nerve growth factor, cholinergic neurons, and spatial learning in rats. J Pharmacol Exp Ther 318:709–724.
30. Schroder N, de Lima MN, Quevedo J, Dal Pizzol F, Roesler R (2005): Impairing effects of chronic haloperidol and clozapine treatment on recognition memory: Possible relation to oxidative stress. Schizophr Res 73:377–378.
31. Ozdemir H, Ertugrul A, Basar K, Saka E (2012): Differential effects of antipsychotics on hippocampal presynaptic protein expressions and recognition memory in a schizophrenia model in mice. Prog Neuropsychopharmacol Biol Psychiatry 39:62–68.
32. Stuchlik A, Rehakova L, Telensky P, Vales K (2007): Morris water maze learning in Long-Evans rats is differentially affected by blockade of D1-like and D2-like dopamine receptors. Neurosci Lett 422: 169–174.
33. Setlow B, McGaugh JL (1998): Sulpiride infused into the nucleus accumbens posttraining impairs memory of spatial water maze training. Behav Neurosci 112:603–610.
34. Bonci A, Hopf FW (2005): The dopamine D2 receptor: New surprises from an old friend. Neuron 47:335–338.
35. Anzalone A, Lizardi-Ortiz JE, Ramos M, De Mei C, Hopf FW, Iaccarino C, *et al*. (2012): Dual control of dopamine synthesis and release by presynaptic and postsynaptic dopamine D2 receptors. J Neurosci 32: 9023–9034.
36. Bello EP, Mateo Y, Gelman DM, Noain D, Shin JH, Low MJ, *et al*. (2011): Cocaine supersensitivity and enhanced motivation for reward in mice lacking dopamine D2 autoreceptors. Nat Neurosci 14: 1033–1038.
37. Turiault M, Parnaudeau S, Milet A, Parlato R, Rouzeau JD, Lazar M, *et al*. (2007): Analysis of dopamine transporter gene expression pattern—generation of DAT-iCre transgenic mice. FEBS J 274: 3568–3577.
38. Giros B, Jaber M, Jones SR, Wightman RM, Caron MG (1996): Hyperlocomotion and indifference to cocaine and amphetamine in mice lacking the dopamine transporter. Nature 379:606–612.
39. Bergson C, Mrzljak L, Smiley JF, Pappy M, Levenson R, Goldman-Rakic PS (1995): Regional, cellular, and subcellular variations in the distribution of D1 and D5 dopamine receptors in primate brain. J Neurosci 15:7821–7836.
40. Ciliax BJ, Nash N, Heilman C, Sunahara R, Hartney A, Tiberi M, *et al*. (2000): Dopamine D(5) receptor immunolocalization in rat and monkey brain. Synapse 37:125–145.
41. Fremeau RT Jr, Duncan GE, Fornaretto MG, Dearry A, Gingrich JA, Breese GR, *et al*. (1991): Localization of D1 dopamine receptor mRNA in brain supports a role in cognitive, affective, and neuroendocrine aspects of dopaminergic neurotransmission. Proc Natl Acad Sci U S A 88:3772–3776.
42. Levey AI, Hersch SM, Rye DB, Sunahara RK, Niznik HB, Kitt CA, *et al*. (1993): Localization of D1 and D2 dopamine receptors in brain with subtype-specific antibodies. Proc Natl Acad Sci U S A 90:8861–8865.
43. Tiberi M, Jarvie KR, Silvia C, Falardeau P, Gingrich JA, Godinot N, *et al*. (1991): Cloning, molecular characterization, and chromosomal assignment of a gene encoding a second D1 dopamine receptor subtype: Differential expression pattern in rat brain compared with the D1A receptor. Proc Natl Acad Sci U S A 88:7491–7495.
44. Kato K, Masa T, Tawara Y, Kobayashi K, Oka T, Okabe A, *et al*. (2001): Dendritic aberrations in the hippocampal granular layer and the amygdalohippocampal area following kindled-seizures. Brain Res 901: 281–295.
45. Andersson RH, Johnston A, Herman PA, Winzer-Serhan UH, Karavanova I, Vullhorst D, *et al*. (2012): Neuregulin and dopamine modulation of hippocampal gamma oscillations is dependent on dopamine D4 receptors. Proc Natl Acad Sci U S A 109:13118–13123.
46. Kwon OB, Paredes D, Gonzalez CM, Neddens J, Hernandez L, Vullhorst D, *et al*. (2008): Neuregulin-1 regulates LTP at CA1

hippocampal synapses through activation of dopamine D4 receptors. Proc Natl Acad Sci U S A 105:15587–15592.
47. Gangarossa G, Longueville S, De Bundel D, Perroy J, Herve D, Girault JA, *et al*. (2012): Characterization of dopamine D1 and D2 receptor-expressing neurons in the mouse hippocampus. Hippocampus 22: 2199–2207.
48. Amaral DG, Scharfman HE, Lavenex P (2007): The dentate gyrus: Fundamental neuroanatomical organization (dentate gyrus for dummies). Prog Brain Res 163:3–22.
49. Jinde S, Zsiros V, Jiang Z, Nakao K, Pickel J, Kohno K, *et al*. (2012): Hilar mossy cell degeneration causes transient dentate granule cell hyperexcitability and impaired pattern separation. Neuron 76: 1189–1200.
50. Scharfman HE, Myers CE (2012): Hilar mossy cells of the dentate gyrus: A historical perspective. Front Neural Circuits 6:106.
51. Descarries L, Watkins KC, Garcia S, Bosler O, Doucet G (1996): Dual character, asynaptic and synaptic, of the dopamine innervation in adult rat neostriatum: a quantitative autoradiographic and immunocytochemical analysis. J Comp Neurol 375:167–186.
52. Rice ME, Cragg SJ (2008): Dopamine spillover after quantal release: Rethinking dopamine transmission in the nigrostriatal pathway. Brain Res Rev 58:303–313.
53. Zoli M, Jansson A, Sykova E, Agnati LF, Fuxe K (1999): Volume transmission in the CNS and its relevance for neuropsychopharmacology. Trends Pharmacol Sci 20:142–150.
54. Gasbarri A, Verney C, Innocenzi R, Campana E, Pacitti C (1994): Mesolimbic dopaminergic neurons innervating the hippocampal formation in the rat: A combined retrograde tracing and immunohistochemical study. Brain Res 668:71–79.
55. Parish CL, Stanic D, Drago J, Borrelli E, Finkelstein DI, Horne MK (2002): Effects of long-term treatment with dopamine receptor agonists and antagonists on terminal arbor size. Eur J Neurosci 16:787–794.
56. Tripanichkul W, Stanic D, Drago J, Finkelstein DI, Horne MK (2003): D2 dopamine receptor blockade results in sprouting of DA axons in the intact animal but prevents sprouting following nigral lesions. Eur J Neurosci 17:1033–1045.
57. Calabresi P, Saiardi A, Pisani A, Baik JH, Centonze D, Mercuri NB, *et al*. (1997): Abnormal synaptic plasticity in the striatum of mice lacking dopamine D2 receptors. J Neurosci 17:4536–4544.
58. Vijayraghavan S, Wang M, Birnbaum SG, Williams GV, Arnsten AF (2007): Inverted-U dopamine D1 receptor actions on prefrontal neurons engaged in working memory. Nat Neurosci 10:376–384.
59. Caley CF, Weber SS (1995): Sulpiride: An antipsychotic with selective dopaminergic antagonist properties. Ann Pharmacother 29:152–160.
60. Ertugrul A, Ozdemir H, Vural A, Dalkara T, Meltzer HY, Saka E (2011): The influence of N-desmethylclozapine and clozapine on recognition memory and BDNF expression in hippocampus. Brain Res Bull 84:144–150.
61. Ploeger GE, Spruijt BM, Cools AR (1992): Effects of haloperidol on the acquisition of a spatial learning task. Physiol Behav 52:979–983.
62. Prokopova I, Bahnik S, Doulames V, Vales K, Petrasek T, Svoboda J, *et al*. (2012): Synergistic effects of dopamine D2-like receptor antagonist sulpiride and beta-blocker propranolol on learning in the carousel maze, a dry-land spatial navigation task. Pharmacol Biochem Behav 102:151–156.
63. Morris RG, Anderson E, Lynch GS, Baudry M (1986): Selective impairment of learning and blockade of long-term potentiation by an N-methyl-D-aspartate receptor antagonist, AP5. Nature 319:774–776.
64. Teather LA, Packard MG, Smith DE, Ellis-Behnke RG, Bazan NG (2005): Differential induction of c-Jun and Fos-like proteins in rat hippocampus and dorsal striatum after training in two water maze tasks. Neurobiol Learn Mem 84:75–84.
65. Agid O, Kapur S, Arenovich T, Zipursky RB (2003): Delayed-onset hypothesis of antipsychotic action: A hypothesis tested and rejected. Arch Gen Psychiatry 60:1228–1235.
66. Holscher C (1999): Synaptic plasticity and learning and memory: LTP and beyond. J Neurosci Res 58:62–75.
67. Kemp A, Manahan-Vaughan D (2004): Hippocampal long-term depression and long-term potentiation encode different aspects of novelty acquisition. Proc Natl Acad Sci U S A 101:8192–8197.
68. Ge Y, Dong Z, Bagot RC, Howland JG, Phillips AG, Wong TP, *et al*. (2010): Hippocampal long-term depression is required for the consolidation of spatial memory. Proc Natl Acad Sci U S A 107: 16697–16702.
69. Goh JJ, Manahan-Vaughan D (2013): Spatial object recognition enables endogenous LTD that curtails LTP in the mouse hippocampus. Cereb Cortex 23:1118–1125.
70. Nicholls RE, Alarcon JM, Malleret G, Carroll RC, Grody M, Vronskaya S, *et al*. (2008): Transgenic mice lacking NMDAR-dependent LTD exhibit deficits in behavioral flexibility. Neuron 58:104–117.
71. Luscher C, Malenka RC (2012): NMDA receptor-dependent long-term potentiation and long-term depression (LTP/LTD). *Cold Spring Harb Perspect Biol* 4(6). pii: a005710.
72. Selcher JC, Xu W, Hanson JE, Malenka RC, Madison DV (2012): Glutamate receptor subunit GluA1 is necessary for long-term potentiation and synapse unsilencing, but not long-term depression in mouse hippocampus. Brain Res 1435:8–14.
73. Peineau S, Nicolas CS, Bortolotto ZA, Bhat RV, Ryves WJ, Harwood AJ, *et al*. (2009): A systematic investigation of the protein kinases involved in NMDA receptor-dependent LTD: Evidence for a role of GSK-3 but not other serine/threonine kinases. Mol Brain 2:22.
74. Peineau S, Taghibiglou C, Bradley C, Wong TP, Liu L, Lu J, *et al*. (2007): LTP inhibits LTD in the hippocampus via regulation of GSK3beta. Neuron 53:703–717.
75. Beaulieu JM, Tirotta E, Sotnikova TD, Masri B, Salahpour A, Gainetdinov RR, *et al*. (2007): Regulation of Akt signaling by D2 and D3 dopamine receptors in vivo. J Neurosci 27:881–885.
76. Lisman JE, Grace AA (2005): The hippocampal-VTA loop: Controlling the entry of information into long-term memory. Neuron 46:703–713.
77. Ho BC, Andreasen NC, Ziebell S, Pierson R, Magnotta V (2011): Long-term antipsychotic treatment and brain volumes: A longitudinal study of first-episode schizophrenia. Arch Gen Psychiatry 68:128–137.
78. Kapur S (2003): Psychosis as a state of aberrant salience: A framework linking biology, phenomenology, and pharmacology in schizophrenia. Am J Psychiatry 160:13–23.